

PORE NETWORK MODEL TO PREDICT FLOW PROCESSES IN UNSATURATED CALCARENITES

NICOLA PASTORE^(*), GIOACCHINO FRANCESCO ANDRIANI^(**), CLAUDIA CHERUBINI^(***),
GIUSEPPE DIPRIZIO^(**), FRANCESCO ANACLERIO^(*), PAOLO MORELLI^(**) & CONCETTA IMMACOLATA GIASI^(*)

^(*)Politecnico di Bari - Dipartimento di Ingegneria Civile, Ambientale, del Territorio, Edile e di Chimica - Bari, Italy

^(**)Università degli Studi di Bari Aldo Moro - Dipartimento di Scienze della Terra e Geoambientali - Bari, Italy

^(***)Dipartimento di Matematica, Informatica e Geoscienze, Università degli Studi di Trieste

Corresponding authors: nicola.pastore@poliba.it, gioacchinofrancesco.andriani@uniba.it

EXTENDED ABSTRACT

La conoscenza dei meccanismi di infiltrazione nella zona vadosa è fondamentale per lo studio della distribuzione spaziale e temporale delle componenti del ciclo idrologico, soprattutto in riferimento ai deflussi sotterranei necessari per la stima della ricarica degli acquiferi. A questo si aggiunge il ruolo importante che assumono i processi di infiltrazione sui meccanismi di instabilità dei pendii, di degradazione di terre e rocce o sull'andamento dei cedimenti nel tempo e sulla valutazione della capacità portante dei terreni di fondazione.

In Puglia e Basilicata (Italia meridionale), è possibile rilevare, sia lungo la costa sia in prossimità del bordo interno delle Murge, estesi affioramenti di roccia calcarenitica plio-quadernaria. Si tratta di facies appartenenti alla Formazione della Calcarenite di Gravina (Pliocene medio-Pleistocene inferiore), costituite principalmente da packstones e grainstones fossiliferi a grana media e ad assetto progradante. La Calcarenite di Gravina poggia con discordanza angolare sul basamento carbonatico del Cretaceo (Formazioni del Calcare di Bari e del Calcare di Altamura) e raggiunge uno spessore variabile da pochi metri a poco più di 50 m; corpi calcarenitici di maggiore potenza caratterizzano l'area di confine tra l'Altopiano delle Murge e l'Avanfossa Bradanica.

Le calcareniti rappresentano un'importante unità idrogeologica che controlla la ricarica delle acque sotterranee e il trasporto dei contaminanti all'interno di un sistema multistrato complesso, comprendente alla base un acquifero profondo costituito dai calcari mesozoici del basamento, permeabili per fratturazione e carsismo.

Una particolarità della formazione calcarenitica è rappresentata dall'estrema variabilità dei caratteri di facies, strettamente connessi ai processi deposizionali e diagenetici, che implicano una differente risposta del materiale in termini meccanici e fisici. Ne consegue un comportamento idraulico complesso, soprattutto in termini di tasso e velocità di infiltrazione e di capacità di ritenzione sia alla scala dell'affioramento sia alla mesoscala. La maggior parte dei modelli di infiltrazione e di ritenzione idrica per mezzi porosi insaturi proposti in letteratura sono basati su rappresentazioni semplificate del sistema dei pori e utilizzano la suzione di matrice come principale variabile di stato.

In questo lavoro, attraverso un approccio metodologico integrato è stato sviluppato uno strumento analitico pratico per lo studio dei meccanismi di infiltrazione e la capacità di ritenzione delle calcareniti. In termini congrui, sono state ricavate relazioni costitutive non parametriche, basate su un modello concettuale dei percorsi di infiltrazione ricavato dalla distribuzione dei pori ottenuta sperimentalmente attraverso una indagine microporosimetrica combinata, utilizzando sia il metodo ad intrusione di mercurio sia l'analisi di immagine. Insieme a test di laboratorio convenzionali e non convenzionali per la caratterizzazione petrofisica del materiale, su concetti di calcarenite, prelevati da un comprensorio di cava, in località *Tufarelle* in agro di Canosa di Puglia, sono state condotte prove di infiltrazione ad anello singolo e a carico variabile alla scala da banco, passando da uno stato secco ad uno umido non prefissato.

Il comportamento idraulico osservato sperimentalmente è ben rappresentato dallo strumento analitico sviluppato. L'analisi comparativa tra il comportamento sperimentale e quello simulato dal modello analitico, ottenuto a partire dalla soluzione dell'equazione di Richards e dalle relazioni costitutive non parametriche tra il contenuto volumetrico d'acqua, la suzione e la conducibilità idraulica, ha dimostrato che la natura bimodale della distribuzione della dimensione dei pori gioca un ruolo fondamentale nella previsione dei meccanismi di infiltrazione e della distribuzione del contenuto volumetrico d'acqua. I modelli semplici basati sull'ipotesi di una distribuzione unimodale dei pori, come il modello di Brooks e Corey, non è in grado di rappresentare il comportamento idraulico delle calcareniti, sebbene fitti molto bene le funzioni non parametriche stimate. Lo studio ha, quindi, evidenziato che ad un grado di saturazione medio alto, nel modello di Brooks e Corey, al diminuire della saturazione effettiva, la conducibilità idraulica diminuisce più rapidamente rispetto al modello non parametrico validato. Ne consegue che l'ipotesi di una distribuzione dei pori unimodale porta ad una errata stima dei meccanismi di infiltrazione e quindi della velocità di propagazione del fronte umido e della distribuzione del contenuto volumetrico di acqua.

I risultati ottenuti da questo studio trovano applicabilità in diversi contesti geologici nell'ambito di tematiche di interesse geingegneristico e ambientale che necessitano di approcci multidisciplinari specifici.

ABSTRACT

The knowledge of infiltration mechanisms in vadose zone is the key to forecast the components of the hydrologic cycle such as run-off generation and aquifer recharge. Besides, slope stability, settlements and bearing capacity of foundations, and rock weathering are issues in which infiltration processes play an important role.

In Apulia and Basilicata (Southern Italy) representative calcarenites outcrops are exposed along both the coastline and internal areas. These calcarenites belong to the Calcarenite di Gravina Fm. (Middle Pliocene-Lower Pleistocene) and are mainly constituted by fine- medium- and coarse-grained packstones and grainstones. The whole geological formation represents an important hydrogeologic unit which controls groundwater recharge and transport of contaminants within a complex, multilayered system comprising a wide and deep aquifer hosted into the Mesozoic basement.

A smart analytical and numerical tool based on the pore bundle model conceptualization and the Richards' equation was developed to predict infiltration and retention mechanism of calcarenites. This work investigated the impact of bimodal pore-size distribution on the unsaturated flow from dry to wet conditions obtained through conventional and unconventional laboratory tests and petrophysical characterization, also completed with mercury intrusion porosimetry and image analysis. Laboratory experiments were carried out on medium-grained grainstones sampled at Canosa di Puglia (*Tufarelle* locality), by means of infiltration tests conducted starting from a different degree of saturation and varying the inlet flow rate. The experimental data were compared with the pore network model prediction.

For the rock samples used, the study disclosed that macroporosity mainly affects the propagation of the wetting front and infiltration rate. Thus, the wetting front develops principally during the infiltration of water through the interconnected macropores following the pathways having minimum flow resistance with a gravity driven flow velocity higher than the diffusive flow through micropores.

KEYWORDS: calcarenite, aquifer, unsaturated flow, pore network model

INTRODUCTION

During the last 70 years, the increasing concern with the infiltration processes for run-off generation, aquifer supply and contaminant transport into vadose zone has stimulated the development of numerous models for describing and/or estimating mechanisms of water retention, transfer and storage (BROOKS & COREY, 1964; CAMPBELL, 1974; COSBY *et alii*, 1984; FREDLUND & XING, 1994; MOREL & NIMMO, 1999; CHEN *et alii*, 2019; ASL *et alii*, 2000; CORRADINI *et alii*, 2011; PASTORE *et alii*, 2020; ANDRIANI *et alii*, 2021). Furthermore, studies on water infiltration rate and mechanisms have found numerous

applications in different fields, including rock/soil deterioration processes, slope stability, settlement and bearing capacity (NG & SHI, 1998; BOWER, 2002; NG & MENZIES, 2007; LU *et alii*, 2009; OH & LU, 2015; XIAO *et alii*, 2016; WANG *et alii*, 2017; CASNEDI *et alii*, 2018; LI *et alii*, 2019; YANG & HUANG, 2023).

The hydraulic behaviour of porous unsaturated soils or rocks is very complex and, all boundary and climatic conditions being equal, is affected by many factors, including mineralogy and fabric of geological media, in terms of texture and microscopic and macroscopic structure. The geometry and topology of the pore network, in fact, controls the ability of soils and rocks to retain or transmit water and is responsible of high non-linearity and spatial variability of the hydraulic parameters governing the transient unsaturated flow (CORRADINI *et alii*, 2002; NIMMO, 2004; ZHAN & NG, 2004; ANDRIANI & WALSH, 2007, 2010; MORBIDELLI *et alii*, 2015; LU, 2018; RANJBAR *et alii*, 2022).

In previous studies some relationships between fabric features and hydraulic behavior or other easily measurable basic physical rock properties were developed (ARYA & PARIS 1981; SAXTON *et alii*, 1986; RUSSO, 1988; WOSTEN & VAN GENUCHTEN, 1988; VERECKEN *et alii*, 1989; EWING & GUPTA, 1993; FREDLUND & XING, 1994; KOSUGI, 1994; FREDLUND *et alii*, 2002; KUTÍLEK, 2004; NIMMO, 2005; MINASNY & MCBRATNEY, 2007; PIRES *et alii*, 2008; NIMMO, 2009; GHAMBARIAN *et alii*, 2010). Relationships between porosity, grain-size, tortuosity of the flow paths and permeability was presented by CARMAN (1937; 1956) and SCHEIDEGGER (1957). The Brooks and Corey power-law function (BROOKS & COREY, 1964) has been widely used as empirical model to predict Soil Water Retention Curves (SWRC), using the "pore-size distribution index", which is a dimensionless parameter related to the curve shapes. The Campbell's equation (CAMPBELL, 1974) represents the moisture retention curve by means of soil moisture content (θ), saturated soil moisture (θ_s), which are both expressed in Vol. %, and air entry potential which depends on pore-size distribution, tortuosity, and connectivity of the porous media. The Van Genuchten empirical model (VAN GENUCHTEN, 1980) is the most widely used for estimating Soil Water Retention Curves of unsaturated soils and rocks. It relates the volumetric water content ($m^3 m^{-3}$) to soil suction, calculated as pressure difference between the air and water phases, by means of two fitting parameters, among which m is dimensionless and, according to VAN GENUCHTEN (1980) and LENHARD *et alii* (1989) can be estimated from the pore-size distribution index of the Brooks and Corey model. Many other empirical models have been developed to describe the Soil Water Retention Curve by means of pore-size distribution and pore space geometry attained applying fractal approaches (TYLER & WHEATCRAFT, 1990; PERRIER *et alii*, 1996; PERFECT *et alii*, 1996; BIRD *et alii*, 2000; XU, 2004; HUANG *et alii*, 2006; FAZELI *et alii*, 2010). Some efforts have been made to estimate hydraulic properties from pedotransfer functions (PTFs) based on basic soil properties such as the particle-size distribution and bulk density (BOUMA, 1989; TIETJE,

1993; WÖSTEN *et alii*, 1995; MINASNY *et alii*, 1999; NEMES & RAWLS, 2004; KHODAVERDILOO *et alii*, 2011; VAN GINKEL & OLSTHOORN, 2019). A qualitative assessment on the incidence of the fabric features affecting physical response and properties including heat and fluid flows have been presented by MORGAN & GORDON (1970), BEARD & WEYL (1973), BRIE *et alii* (1985), HOFFMAN & NIESEL, (1996), CAPUTO *et alii* (1996), ANDRIANI & WALSH (2002).

Many models and techniques used to obtain the Soil Water Retention Curve remain difficult, poor practical and time-consuming. Furthermore, they show limited applicability being almost exclusively focused on soils characterised by primary porosity. The continuous and open space system of rocks is more complex and comprises both pores and fracture voids or cavities. The presence of pervasive discontinuities in rock masses, in fact, influences the hydraulic behavior of media and the fracture-dominated flow. In addition, for rock materials is not so simple to realize and install technical devices, both *in situ* and *ex situ*.

Not surprisingly, the international literature concerning the assessment of the hydraulic properties of rocks is quite limited and based on adaptive applications of standard methods and/or analytical approaches by means of theoretical studies and numerical simulations generally used for soils (NIMMO *et alii*, 1987; SCHNEEBELI, 1995; REYNOLDS *et alii*, 2002; ZHOU *et alii*, 2004; CASTIGLIONE *et alii*, 2005; AMERICAN SOCIETY FOR TESTING AND MATERIALS, 2008; CAPUTO *et alii*, 2010, 2012; AMARASINGHE *et alii*, 2011; LU *et alii*, 2011; LIU & XU, 2017; ANDRIANI *et alii*, 2021).

In this work, through an integrated methodological approach, a practical analytical tool was developed for the study of the unsaturated hydraulic behaviour of calcarenites, in terms of the unsaturated hydraulic conductivity function and Soil Water Retention Curve. Calcarenite ashlar, taken from the quarry district of *Tufarelle* at Canosa di Puglia, Apulia (South Italy), was used as experimental material (Fig. 1).

Together with conventional and non-conventional laboratory tests for the petrophysical characterization of the material, single ring infiltration tests under falling head conditions were conducted at bench scale, passing from dry to non-predetermined wet state. A

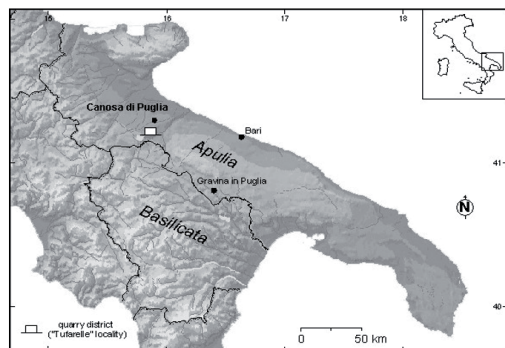


Fig. 1 - Location map showing the calcarenite extraction site of Tufarelle, Canosa di Puglia (Apulia, South Italy)

combined microporosimetric investigation, using both the mercury intrusion method and image analysis, was used for characterizing the complex pore network and the pore grading of the calcarenite. Non-parametric constitutive relations were found, based on a conceptual model of the infiltration paths obtained from the pore-size distribution, tortuosity and structure of the porous media. The results obtained from this study find applicability in different geological contexts for a number of geo-engineering and environmental topics which require specific multidisciplinary approaches.

MATERIAL AND METHODS

In Apulia and Basilicata (Southern Italy) representative calcarenites outcrops are exposed along both the coastline and internal areas. These calcarenites belong to the Calcarenite di Gravina Fm. (Middle Pliocene-Lower Pleistocene) and are mainly constituted by well sorted medium-grained fossiliferous packstones and grainstones, massive or stratified with prograding geometry. The Calcarenite di Gravina Fm. unconformably lies on the Cretaceous calcareous basement (Calcere di Bari and Calcere di Altamura Fms.) and is characterised by a thickness ranging from few decimeters up to over 50 m; the maximum thickness is found at the border area between the Murge plateau and the Bradanic Foredeep (TROPEANO & SABATO, 2000). The calcarenites represents an important hydrogeologic unit because they control groundwater recharge and transport of contaminants within a complex, multilayered system which comprises a wide and deep aquifer hosted into the Mesozoic basement. In fact, a peculiarity of the calcarenites is represented by the extreme variability in the rock-fabric/petrophysical characteristics, closely connected to the depositional and diagenetic processes. All that implies both changing mechanical properties of the material and complex hydraulic behavior, especially in terms of infiltration rate and capacity or hydraulic conductivity and retention capability, at the outcrop scale or mesoscale.

For this study, quarry ashlar of calcarenite were sampled at Canosa di Puglia (*Tufarelle* locality) (Fig. 2). Field description and microscopic analysis on standard thin sections by means of transmitted light microscopy were carried out (Fig. 3).



Fig. 2 - Panoramic view of the Tufarelle quarry (Canosa di Puglia, Apulia - South Italy)

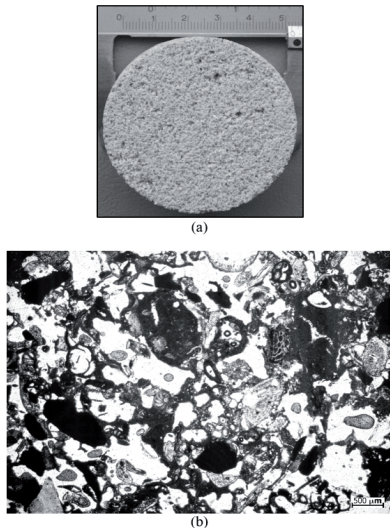


Fig. 3 - Mesoscopic aspect (a) and microscopic appearance in plane-polarized light on standard thin-sections using polarizing microscopy of the calcarenite tested in this study (b)

According to FOLK (1959, 1962) the calcarenite can be classified as a biointrasparite, whilst according to DUNHUM (1962) it is a grainstone. Bioclasts and intraclasts are well sorted mainly in the range 0.1-2.0 mm and arranged chaotically with low packing density. It follows an open texture in which all pores are interconnected and accessible. They are intergranular in type, but also intragranular and moldic pores in combination with inter-crystalline and microfracture porosity reflect high effective porosity and water transmissivity of this material. The content in cement is few. It is carbonatic in origin and is irregularly distributed in the rock. Microcrystalline meniscus-type cements at grain contact or on the grain walls in open pore spaces or also in the inner cavities of bioclasts represent the main type of cementation in the rock. Sparry calcite is very rare and never totally fills the intergranular and intragranular pore spaces.

According to the standard test procedure outlined in the International SOCIETY FOR ROCK MECHANICS (1979), some basic physical properties were determined on fresh calcarenite samples. Saturated density, degree of saturation and water absorption were estimated according to ANDRIANI & WALSH (2002; 2007). The data obtained are summarised in Table 1.

Grain size analysis was performed on loose material obtained from saturated specimens subjected to freeze-thaw cycles and disaggregated by hand to avoid breaking of bioclasts and lithoclasts. Sieve and sedimentation techniques were used. The results of the grain-size analysis were graphically represented in the form of grading envelope of 18 samples (Fig. 4).

According to ASTM D4404 (1984), the MIP was performed for determining pore-size distribution (PSD), effective porosity (26%), mean and median pore diameter (6.03 μm and 12.96 μm), and tortuosity (1.925). A Micromeritics porosimeter

Physical property	Calcarenite		
	Tufarelle loc., Apulia-Italy		mean
	min	max	
Specific gravity, G_s		2.70	
Dry density, ρ_d (Mg/m ³)	1.34	1.58	1.45
Sat. density, ρ_{sat} (Mg/m ³)	1.84	2.04	1.91
Porosity, n (%)	41.5	50.4	46.5
Water absorption, w_a (%)	26.3	37.6	32.3
Degree of saturation, S_r (%)	100	100	100

Tab. 1 - Physical properties of the calcarenite tested.

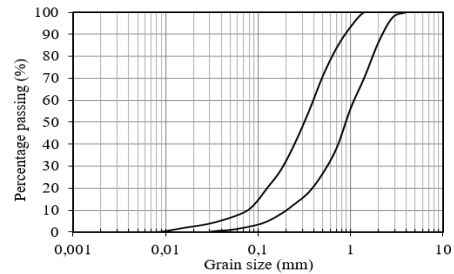


Fig. 4 - Grading envelope obtained for the Tufarelle calcarenite, Canosa di Puglia - Apulia, Italy

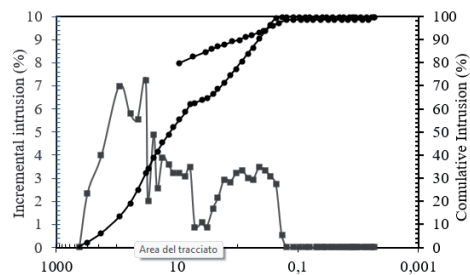


Fig. 5 - Pore size distribution obtained by MIP measurements for the Tufarelle calcarenite, Canosa di Puglia - Apulia, Italy

(Autopore IV 9500) was used at low pressure (3.44-345 kPa) and high pressure (0.1-228 MPa) on calcarenite fragments of irregular shape of about 2.5 g. Within the limitation of the operative conditions and the applied methodology, the MIP technique allowed to evaluate the pore size distribution and the relative porosity for pores with a diameter between 0.0055 and 420 micrometers. The results of the MIP analysis were graphically represented in the form of cumulative and incremental intrusion vs. pore-size diameter curves (Fig. 5). To investigate the distribution also of pores greater than 420 micrometers, Image Analysis (IA) technique was performed on photo-micrographs of thin-sections in plane-polarised light transferred directly on a PC. Twenty-five photo-micrographs were used for the analysis.

According to FRANCUS (1998), PSD by image analysis was carried out as distribution of the “equivalent-disk diameter”. It is important to highlight that the minimum size for objects was fixed and depends on the resolving power of the image-digitizing equipment (20 micrometers). Pore size distribution generated from image data was viewed as pore count frequency which gives equal weight to individual pores regardless of their size. According to IA measurements, the highest pore count frequency was recorded in the range 1,000-75 μm (Fig. 6).

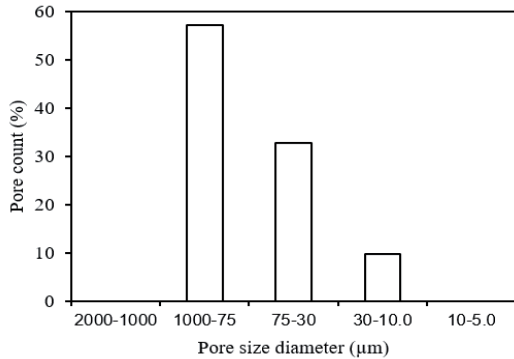


Fig. 6 - Pore size distribution obtained by IA measurements for the Tu-farelle calcarenite, Canosa di Puglia - Apulia, Italy

Theoretical background

The fluid flow through variability saturated geological media, under the assumption that the different pore regions (macropore and micropore) are in equilibrium, can be described by the Richard’s equation:

$$C(\theta) \partial\psi/\partial t = \nabla \cdot [K(\theta) (\nabla\psi + \nabla z)] \tag{1}$$

where ψ (m) is the matric head, θ (m^3m^{-3}) is the volumetric water content, $C(\theta)$ (m^{-1}) is the water capacity equal to the derivative of θ with respect to ψ , and $K(\theta)$ (ms^{-1}) is the hydraulic conductivity as function of the volumetric water content.

Neglecting the residual water content θ_r (m^3m^{-3}), the volumetric water content θ is equal to the product between the saturated volumetric water content θ_s (m^3m^{-3}) and the effective saturation Se (-), whereas $K(\theta)$ is equal to the product between the saturated hydraulic conductivity K_s (ms^{-1}) and the relative hydraulic conductivity function $k_r(\theta)$ (-).

In order to solve Equation 1, constitutive relationships between the matric head, volumetric water content, effective saturation and relative hydraulic conductivity are needed.

Brook and Corey model (XING *et alii*, 2016), based on the assumption of the existence of the air entry pressure, can be used to predict the Soil Water Retention Curve and the hydraulic conductivity:

$$\theta = \theta_s Se = (\psi_d / \psi)^n \tag{2}$$

$$k_r(\theta) = (\theta / \theta_s)^{3+2/n} = Se^{3+2/n} \tag{3}$$

where, ψ_d [m] is the air entry pressure head and n [-] is an empirical parameter.

Alternatively, once known the pore size distribution (PSD) of the geological medium it is possible determine the constitutive relationships (relation between volumetric water content and matric head, relation between relative hydraulic conductivity and volumetric water content) (NOVOTNY *et alii*, 2023; CHEN & CHEN,

2020). Capillarity represents the main retention mechanism in an unsaturated geological medium between wet and moderately wet stage. Capillarity favors the saturation of small pores at given matric head. Then, at a given volumetric water content θ_i (m^3m^{-3}) there exists a critical pore diameter d_i (m) whether the pores having are filled with water. Then the matric head ψ , effective saturation Se , and relative hydraulic conductivity k_r can be obtained as function of the critical diameter d_i .

The capillary mechanism can be expressed by the Young – Laplace equation where the matric head ψ_i at which a pore fills or empty is function of the correspondent critical pore diameter d_i :

$$\psi_i(d_i) = \sigma \cos \varepsilon / d_i \rho_w g \tag{4}$$

Where σ is the surface tension (Nm^{-1}), ε (-) is the contact angle between particles and water, ρ_w is density of water (kgm^{-3}), and g (ms^{-2}) is the gravity acceleration. According to MOHAMMADI & VANCLOOSTER (2011) and CHANG & CHENG (2018), the contact angle ε is equal to 0.

According to the pore bundle concept, the pore network can be depicted as a cluster of tortuous capillary tubes with smooth inner surface. On the basis of this concept, ANDRIANI *et alii* (2021) derived the following relationship between the critical pore diameter and effective saturation:

$$Se(d_i) = \sum_{j=1}^i d_j^2 / \sum_{j=1}^n d_j^2 \tag{5}$$

and between the critical pore diameter and the relative hydraulic conductivity:

$$k_r(d_i) = \sum_{j=1}^i d_j^{3+D_i} / \sum_{j=1}^n d_j^{3+D_i} \tag{6}$$

where D_i (-) is the tortuosity fractal dimension variable between 1 and 2 (FENG & YU, 2007).

Falling Head Infiltration Tests At Bench Scale

On regularly shaped prisms (ashlars) of calcarenite rock with $L = 39.5$ cm, $W = 24.5$ cm, and $H = 14.5$ cm. A set of 3 ashlar was used in the experiments. The procedure used included drying of the material at 110° C in an oven for 24 h.

A clear polycarbonate cylinder with diameter (D) of 12.0 cm and height of 50.0 cm was positioned in perfect central position on the top surface of the ashlar to depth of about 0.2 cm into the rock for ensuring good rock–cylinder contact. The cylinder was then sealed with water-proof cement-bentonite material to prevent lateral outflow of water. The cylinder was filled to the top with de-aired water to a given level and a few drops of oil were added on the water surface to prevent water from evaporating. At the beginning of the test, a water level of about $h_0 = 25$ cm was fixed for each test. Water level in the cylinder was allowed to lower between 13 and 15 cm. The water level fall $h(t)$

was measured over time with a ruler. The testing time ranged from 30 to 40 minutes. The room temperature was 20 ± 1.0 °C, while the test water temperature was 15 ± 1 °C. No changes in temperature were registered during each test. Advancement of the lateral wetting front was first observed only on the top surfaces of the ashlars, growing like a spiral concentric circle geometry model. Later, after a few minutes, the moisture plume appeared also on the fair-faced side of the ashlars. Wetting front traces along the faces were also measured over time with a ruler.

According to procedure described in ANDRIANI *et alii* (2021), the geometric volume of the moisture plume V_g (m³) as well as the coordinates along the vertical direction of the centroid of the wetting front Z_g were determined. Then the average effective saturation of the moisture plume was determined as:

$$\bar{S}_e = \frac{V_{in}}{V_g \theta_s} \quad (7)$$

where V_{in} (m³) is the total water volume entered into the rock.

Figure 7 shows a sketch of the experimental setup.

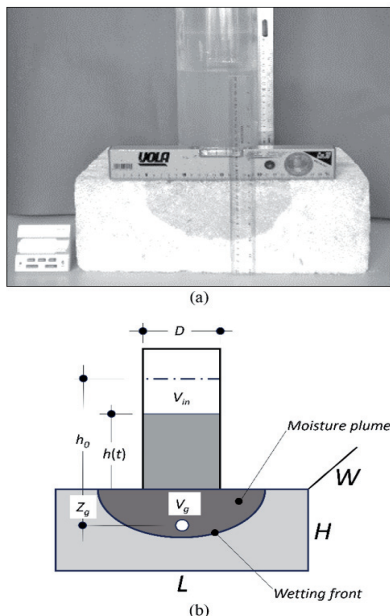


Fig. 7 - View of the falling head infiltration setup on a calcarenite ashlar used in this study (a); schematic diagram of the falling head infiltration test at bench scale (b)

RESULTS

Pore-size distribution

The estimation of the relative hydraulic conductivity and Soil Water Retention Curve from the pore bundle conceptual model requires an accurate estimate of the pore-size distribution (PSD). Starting from the data obtained by both MIP and IA, a representative evaluation of the total pore-size distribution for the material was modelled by means of a Monte Carlo simulation

(ANDRIANI *et alii*, 2021). Figure 8 (a) shows the cumulative pore volume frequency curve derived from the application of the Monte Carlo method. The relative frequency histogram is shown in Figure 8 (b). The pore sizes obtained with this method range from 0.19 μm to about 1,000 μm with a typical bimodal distribution around the 1,000-75 μm and 1.0-0.01 μm mode classes.

The incremental mercury intrusion data vs. pore-size diameter demonstrated that a bimodal trend occurs in the throat-size distribution of the material in correspondence of 0.43 μm and 6.03 μm (Fig. 5).

Hydraulic behaviour of unsaturated calcarenite

Figure 9 shows the non-parametric SWRC derived according to the PSD of calcarenite, and the correspondent Brooks and Corey fitted model. Starting from full saturation conditions, the drainage process starts when the matric head become lower than the air entry. The water within macropores drains first and the volumetric water content decreases. A change of slope in the SWRC is evident in correspondence of the matric head (ψ) of -10 m and the volumetric water content (θ) of 0.099 (Fig. 9). For lower values of θ and higher values of ψ , macropores are empty and micropores govern the drainage process ($d_i < 5 - 10$ μm).

Consequently, the volumetric water content decreases more slowly. Even if the Brooks and Corey model well fits the SWRC derived from PSD, it fails to represent the bi-modal characteristics of the non-parametric SWRC.

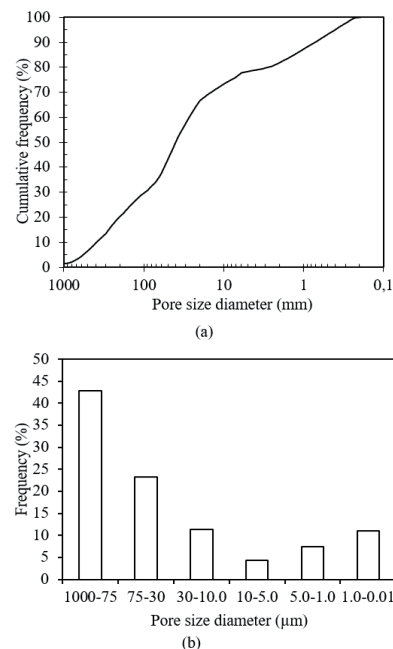


Fig. 8 - Cumulative pore volume frequency curve (a) and relative frequency histogram (b) for the Tufarelle calcarenite obtained by combining MIP and IA data with a Monte Carlo simulation (ANDRIANI & WALSH, 2002; ANDRIANI *et alii*, 2021)

An early rapid drop of the water level in the cylinder was observed during the falling head infiltration test at bench scale due to the rapid infiltration of water in dry calcarenites. When the water level drop reaches the value of 0.078 m at 540 s a steady state water infiltration rate is disclosed which shows an average value determined according to the volumetric method of $6 \times 10^{-5} \text{ ms}^{-1}$.

Figure 10 shows the average effective saturation, Se , of the moisture plume versus time.

In the early stage, the moisture plume propagates in saturated conditions and air in the pores is completely replaced by water. The geometric volume of the moisture plume V_g approaches the value of the total water volume into the rock V_{in} . Successively, for a time higher than 365 s, V_{in} becomes lower than its initial value and unsaturated condition occurs with a value of the measured average effective saturation between 96.29 % and 51.78 %.

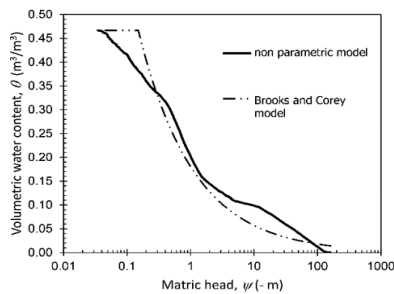


Fig. 9 - Estimated non-parametric Soil Water Retention Curve (SWRC) derived applying the Montecarlo method and the correspondent Brooks and Corey fitted model with $\psi_d = -0.15$ and $n = 0.5$

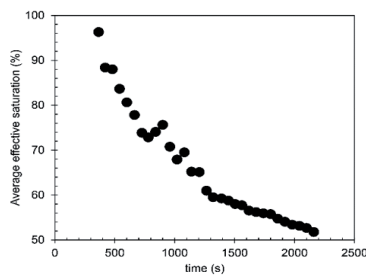


Fig. 10 - Average effective saturation versus time

In order to validate the pore bundle model (eqs 5 and 6), the observed and predicted behaviour of the evolution of the moisture plume was compared. In particular, the observed evolution of the centroid of the wetting front Z_G was fitted with its predicted value Z'_G , calculated, according to ANDRIANI *et alii* (2021), as the time integral of the derivative of the hydraulic conductivity respect to water volume content:

$$Z'_G = \int \frac{dK}{d\theta} dt = \frac{K_s}{\theta_s} \int \frac{dk_r}{dSe} dt \quad (8)$$

The values of the derivative of the relative hydraulic conductivity with respect to the effective saturation were

determined in correspondence of the values of the average effective saturation.

Figure 11 shows the comparison between observed and predicted values. The predicted model shows a satisfactory fitting, closing the experimental data for a value of the saturated hydraulic conductivity of $5.50 \times 10^{-5} \text{ ms}^{-1}$ and a value of the tortuosity fractal dimension of $D_f = 1.20$.

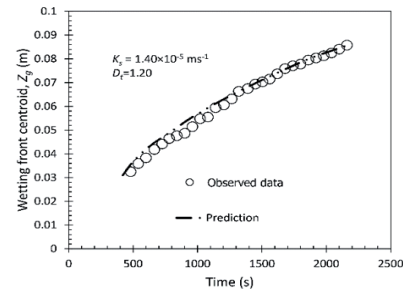


Fig. 11 - Vertical coordinate of the centroid of the wetting front versus time and its predicted value estimated with equation 8

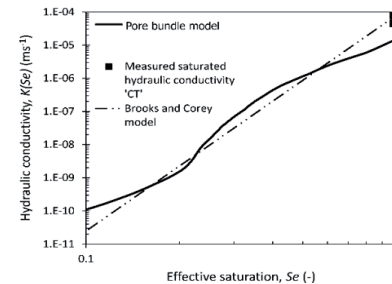


Fig. 12 - Estimated non-parametric hydraulic conductivity function estimated according to the pore bundle model and the correspondent Brooks and Corey fitted model with $K_s = 7.88 \times 10^{-5} \text{ ms}^{-1}$

Figure 12 shows the non-parametric hydraulic conductivity function estimated through the pore bundle model. When the effective saturation becomes lower than 0.27, macropores characterized by a diameter d_i higher than 5-10 μm result empty, and do not contribute to the water flow. As a consequence, the relative hydraulic conductivity decreases rapidly. As expected, the dual porosity behaviour of the non-parametric K - Se curve is not predicted by the corresponding Brooks and Corey fitted model.

In order to demonstrate the implications of the theoretical and experimental results on practical engineering geology problems, pore bundle model and the relative Brooks and Corey fitted model are compared on a one-dimensional benchmark infiltration problem. Then Richard's equation (Eq. 1) is solved by finite element numerical scheme using the software COMSOL Multiphysics 4.0a (COMSOL Multiphysics®, 2010).

Model domain presents length along the coordinate z of 1 m. It is discretized by finite elements of length of 0.005 m. The initial volumetric water content is null. At $z = 0$ a flux boundary condition is imposed corresponding to a constant

rainfall event of 40 mmh^{-1} for a time of 1 hour.

Figures 13 and 14 show the volumetric water content distribution along the depth after 5 hours from the rainfall events and the volumetric water content breakthrough curve at depth of 0.1 m respectively for both models.

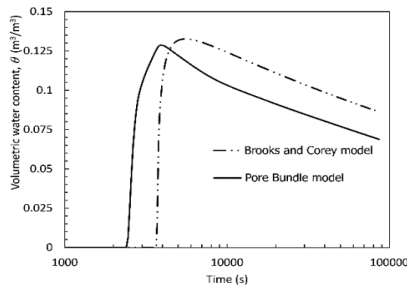


Fig. 13 - Breakthrough curve of the volumetric water content at depth $z = 0.1 \text{ m}$ for both pore bundle model and Brooks and Corey model

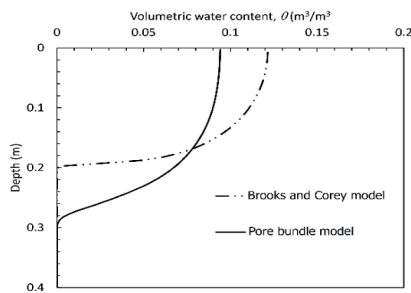


Fig. 14 - Volumetric water content distribution along the depth after 5 hours from the rainfall event for both pore bundle model and Brooks and Corey model

The pore bundle model predicts a more rapid infiltration of the water in the calcarenite rock than the Brooks and Corey model. Then the wetting front is characterized by a lower volumetric water content reaching greater depth (Fig 14). Notwithstanding the saturated hydraulic conductivity value for Brooks and Corey fitted model is higher than the pore bundle model, the infiltration velocity of the latter is higher. As shown in Figure 13, the first arrival of BTC curve of the Brooks and Corey model present a delay respect to the BTC of the pore bundle model of 21 minutes.

DISCUSSION

The goal of this study is to predict the unsaturated hydraulic behaviour of calcarenites by means of theoretical conceptual model analysis, conventional and unconventional laboratory tests, including single-ring infiltration experiments, and numerical modeling.

Pore network and structure

With few exceptions, all the lithofacies belonging to the Calcarenite di Gravina Fm. are characterised by open porosity with interconnected pores. At the rock mass scale, two components of porosity can be considered: textural and structural.

The textural porosity depends on particles arrangement and interlocking, and the nature of individual grains (bioclasts and species types, lithoclasts etc.); the structural porosity, on the other hand, is linked to the presence of macroscopic non-random discontinuities, e.g. fractures, faults and karst features (ANDRIANI & PARISE, 2015, 2017). At the mesoscopic scale, the porosity of calcarenites is essentially textural in type, and structural porosity is confined to the presence of sedimentary structures, bioturbations and microcracks.

In this study, the material tested is represented by a grainstone composed by bioclasts and lithoclasts with different shapes and roundness, and lower packing density with respect to a theoretical arrangement of spherical grains having the same grain-size distribution. This lithofacies, in fact, is not organized according to the most closed arrangement because compaction was inhibited by an early-stage carbonate cementation which is the dominant type of cement of the rock. As a consequence, the porosity calculated by traditional geotechnical procedures is high and open (all pores are interconnected and accessible). Then, intergranular, intragranular and moldic porosity in combination with inter-crystalline and microfracture porosity reflect high effective porosity and water transmissivity of these materials. According to the pore-size classification by BREWER (1964), if intergranular pores can be considered almost all macropores of uniform size but different shapes, the other types of pores are characterised by heterogeneous pore-size distributions and different shapes. In particular, moldic pores are mainly subspherical and range from 30 to 350 micrometers, intragranular pores are different in size and shape according to the species types of the bioclastic fraction, while inter-crystalline pores and microcracks are mainly represented by tortuous micro-throats. Inter-crystalline pores develop inside cements, while microcracks affect also bioclasts, especially microforaminifers.

The pore network of the calcarenites can be schematically considered as a system of pseudo-spherical and tetracubic voids directly connected by cylindrical tubes or neck-shaped channels. Pore-size distribution is thus heterogeneous because the first type of pores are macropores, cylindrical tubes are macro- or mesopores, while neck-shaped channels are more tortuous and mainly microporous, and in part mesoporous in nature. It is principally a texture porosity in which macropores and mesopores, which constitute the prevailing pore fractions, are connected by micro-throats.

Infiltration behaviour at the bench scale

The study of the infiltration processes in soil are commonly based on Richards' flow model in which the flow processes are governed by gravity and capillary force. Constitutive relationships between matric head, water content and hydraulic conductivity are commonly described by BROOKS & COREY (1964) and VAN GENUCHTEN (1980) models which reflect a unimodal pore-size distribution of the porous media. As disclosed in the present work,

the calcarenite tested is characterized by a bi-modal pore-size distribution. Then this geological medium can be viewed as at least two interactive regions, one associated with the presence of macropores and mesopores, the other associated with micropores. Anyway, as demonstrated, equilibrium conditions between micropores and meso-macropores region can be still considered valid. Under this hypothesis, water retention model for dual porosity media can be derived through its pore-size distribution, where the bi-modal PSD can be obtained by superimposing the PSDs of the micropore and meso-macropore regions to estimate bi-modal water retention curve. CHEN & FENG (2023) reach the same conclusion in Nanyang clay characterized by bi-modal pore-size distribution.

Falling head infiltration test highlights an infiltration rate of $6 \times 10^{-5} \text{ ms}^{-1}$ which is consistent with the value of $3 \times 10^{-5} \text{ ms}^{-1}$ observed in single ring infiltrometer field test on the same medium-grained grainstone (ANDRIANI *et alii*, 2013).

The experimental observation of the wetting front growth during the falling head infiltration test at bench scale shows that the geometric volume of the moisture plume increases more than proportionally to the total water volume entered into the rock. As consequence, the average effective saturation is below 100%. This means that water infiltrates more quickly through interconnected larger pores by passing several meso- and macropores to which are connected by micro-throats. For this reason, a number of meso- and macropores can remain dry during infiltration of water. Thus, inlet flow rate is higher than infiltration rates through the smallest meso- and micropores which, due to the gradient of the matric potential, absorb water until they are filled. Then once the smaller pores are filled and consequently the matric head decreases, water moves through the remaining meso- and macropores.

The infiltration behaviour observed in the bench scale single ring test is well represented by the pore bundle model according to a value of the tortuosity fractal dimension (D) equal to 1.2 and a value of saturated hydraulic conductivity of $5.55 \times 10^{-5} \text{ ms}^{-1}$. The non-parametric soil water retention and hydraulic conductivity functions derived by the pore bundle concept depict the textural features of the calcarenite tested. The simple Brooks and Corey fitted model is not able to represent the hydraulic behaviour of such material: by decreasing effective saturation, hydraulic conductivity decreases more rapidly in the Brook and Corey fitted model than in the non-parametric model. The smallest pores are filled, and water develops by means of a continuous flow through interconnected macropores or meso- and macropores, following flow paths characterized by the minimum flow resistance.

For a value of the effective saturation around 0.2, corresponding to a value of matric head around of -10 m, the behaviour of the two models is reversed. Macropores results empty and drainage processes is governed by micropores. Consequently, diffusive mixing mechanism is higher than the gravity driven flow.

Laboratory experimental investigations based on soil suction,

measurements at different volumetric content (TURTURRO *et alii*, 2013) and quasi-steady centrifuge method (TURTURRO *et alii*, 2020) on samples belonging to this lithofacies found similar behaviour on experimental SWRC and hydraulic conductivity functions.

The experimental hydraulic conductivity functions obtained in this study are coherent with the results presented in CAPUTO & NIMMO (2005). In fact, according to these authors, the hydraulic conductivity functions, determined for a calcarenite type comparable to that used in our study, show the same behaviour for the volumetric water content range investigated.

Infiltration behaviour at the field scale

The existence of dual porosity for this type of material influences the prediction of the wetting front propagation and moisture content in the field application. A faster propagation of the wetting front during rainfall event with respect to the value that could be obtained under the assumption of the unimodal pore-size distribution represented by the Brooks and Corey model is disclosed. As shown in Figure 15, at depth of 0.1 m a delay of 21 minutes of the first arrival of the BTC of the Brooks and Corey fitted model with respect to the pore bundle model is highlighted. This means that as the scale of observation, the difference between the two models becomes more relevant. Therefore, the textural characteristics and the relative hydraulic features of such geological media must be considered in order to have a more accurate estimation of the wetting front propagation and moisture content which affect many geo-engineering problems related to hydrologic cycle, contaminant propagation and slope stability.

CONCLUSIONS

Over the last 70 years, many theoretical and empirical models have been developed for deriving the constitutive relationships between volumetric water content, matric head and hydraulic properties of unsaturated geological media. One of the main limitations of these models regards the assumption of a unimodal pore-size distribution. Several lithofacies are characterized by a bimodal pore-size distribution due to fabric features, in terms of textural and structural characteristics at different scales.

In particular, by means of an integrated approach, comprising experimental, conceptual, theoretical, and numerical analyses, this study demonstrated that for calcarenites it is fundamental a detailed estimation of the topology of the pore network and the pore-size distribution to assess the moisture content profile, infiltration mechanisms and water infiltration velocity. The gravity-driven flow mainly through the macropores under strong inflow conditions and high infiltration rate resulted faster than the diffusive flow mainly through the micropores.

Limitations of this study include:

- a) Equilibrium conditions between meso-macropore and micropore regions;

b) Only gravity driven flow and capillarity forces have been considered, neglecting the contribution of “special flow modes” (*sensu* TURTURRO *et alii*, 2020), especially likely in partially filled macropores;

c) The theoretical model has been validated for medium-high degree of saturation ($S_e > 0.5$) and high values of the inlet flow rate of water.

In the next future, new boundary conditions will be adopted in the experimental setup, varying the initial degree of saturation and the infiltration rate. In situ experiments will be used to validate the development of conceptual models also at

field scale. The validity of the equilibrium condition will be investigated comparing reliability of different conceptual models to represent the complex porous structure of calcarenites.

ACKNOWLEDGMENTS

This research was financially supported by European Community within the Project Interreg III A “WET SYS B” 2000-2006 (responsible G.F. Andriani) and Apulia Region within the Program “CT14” (responsible G.F. Andriani).

The authors would like to acknowledge the Network for Energy Sustainable Transition (NEST) for supporting research activities.

REFERENCES

- AMARASINGHE R., WATANABE K. & MAUNG MAUNG M. (2011) - *Estimating unsaturated hydraulic properties of soft rock by three different flow model*. J. Jpn. Soc. Civ. Eng., Ser., **4**(1): 91-96.
- AMERICAN SOCIETY FOR TESTING AND MATERIALS (ASTM) D6527 (2008) - *Standard Test Method for Determining Unsaturated and Saturated Hydraulic Conductivity in Porous Media by Steady-State Centrifugation (Withdrawn 2017)*. ASTM International, West Conshohocken, PA.
- AMERICAN SOCIETY FOR TESTING AND MATERIALS (ASTM) D4404 (1984) - *Standard Test Method for Determination of Pore Volume and Pore Volume Distribution of Soil and Rock by Mercury Intrusion Porosimetry*. ASTM International, West Conshohocken, PA.
- ANDRIANI G. F. PASTORE N., GIASI C.I. & PARISE M. (2021) - *Hydraulic properties of unsaturated calcarenites by means of a new integrated approach*. Journal of Hydrology, Volume **602**: 126730. <https://doi.org/10.1016/j.jhydrol.2021.126730>.
- ANDRIANI G.F. & PARISE M. (2017) - *Applying rock mass classifications to carbonate rocks for engineering purposes with a new approach using the rock engineering system*. J. Rock Mech. Geotech. Eng., **9**(2): 364-369.
- ANDRIANI G.F. & PARISE M. (2015) - *On the applicability of geomechanical models for carbonate rock masses interested by karst processes*. Environ. Earth Sci., **74**(12): 7813-7821. <https://doi.org/10.1007/s12665-015-4596-z>.
- ANDRIANI G.F., LUPARELLI F. & QUARTO R. (2013) - *Water infiltration in unsaturated calcarenites*. Rend. On. Soc. Geol. Ital., **24**: 15-18.
- ANDRIANI G.F. & N. WALSH (2010) - *Petrophysical and mechanical properties of soft and porous building rocks used in Apulian monuments (south Italy)*. Geol. Soc. London Spec. Publ., **333**: 129-141.
- ANDRIANI G.F. & N. WALSH (2007) - *The effects of wetting and drying, and marine salt crystallization on calcarenite rocks used as building material in historic monuments*. Geol. Soc. London Spec. Publ., **271**: 179-188.
- ANDRIANI G.F. & WALSH N. (2002) - *Physical properties and textural parameters of calcarenitic rocks: qualitative and quantitative evaluations*. Eng. Geol., **67**: 5-15.
- ARYA L. M. & PARIS J. F. (1981) - *A physicoempirical model to predict the soil moisture characteristic from particle size distribution and bulk density data*. Soil Sci. Soc. Am. J., **45**: 1023-1030.
- ASL R.H., SALMASI F. & ARVANAGHI H. (2020) - *Numerical investigation on geometric configurations affecting seepage from unlined earthen channels and the comparison with field measurement*. Eng. Appl. Comput. Fluid Mech., **14**(1): 236-253.
- BEARD D.C. & WEYL P.K. (1973) - *Influence of texture on porosity and permeability of unconsolidated sand*. AAPG Bull., **57**: 349-369.
- BIRD N. R. A., PERRIER E. & RIEU M. (2000) - *The water retention function for a model of soil structure with pore and solid fractal distributions*. Eur. J. Soil Sci., **51**: 55-63.
- BOUMA J. (1989) - *Using soil survey data for quantitative land evaluation*. Adv. Soil Sci., **9**: 177-213
- BOWER H. (2002) - *Artificial recharge of groundwater: hydrogeology and engineering*. Hydr. Jour., **10**: 121-142.
- BREWER R. (1964) - *Fabric and Mineral Analysis of Soils*. J. Wiley and Sons, New York.
- BRIE A., JOHNSON D. L. & NURMI R. D. (1985) - *Effect of spherical pores on sonic and resistivity measurements*. Trans. SPWLA Annu. Logging Symp., **26** (1), WI-520.
- BROOKS R. H. & A. T. COREY (1964) - *Hydraulic properties of porous media*. Hydrol. Pap., Vol. **3**, Colo. State Univ., Fort Collins: 37 pp.
- CAMPBELL G.S., (1974) - *A simple method for determining unsaturated conductivity from moisture retention data*. Soil Sci., **117**: 311-314.
- CAPUTO M.C., DE CARLO L. & MASCIALE R. (2012) - *Hydrogeophysical approach to measure hydraulic parameters on unsaturated rocks*. Fresenius Environ. Bull. **21**: 3077-3082.
- CAPUTO M.C., DE BENEDICTIS F., MASCIALE R. & PARILKOVA J. (2010B) - *Electrical impedance spectrometry method to measure rock water content in laboratory*. In CD, Valencia IAHR, International groundwater symposium, 22-24 September 2010. neuv. Valencia, Universidad Politecnica De Valencia. 2010: 1-13.
- CAPUTO M.C., DE CARLO L., MASCIOPINTO C. & NIMMO J. R. (2010A) - *Measurement Of Field-Saturated Hydraulic Conductivity On Fractured Rock Out-*

- crops Near Altamura (Sothorn Italy) With An Adjustable Large Ring Infiltrometer.* Environment Earth Sci., **60**: 583-590.
- CAPUTO M.C., DE CARLO L. & DE BENEDETTIS F. (2010C) - *Evaluation of flow rate in unsaturated rock: field test with integrated approach.* Fresenius Environmental Bulletin, **19**: 1963-1970.
- CAPUTO M.C., QUADRATO E. & WALSH N. (1996) - *Influenza dello shock termico sui parametri fisico-meccanici del "Tufo Calcarea" del bordo occidentale delle Murge.* Mem. Soc. Geol. Ital., **51**: 813-822.
- CARMAN P.C. (1956) - *Flow of gases through porous media.* Academic Press Inc., New York: 182 pp.
- CARMAN P.C. (1937) - *Fluid flow through granular beds.* Trans. Inst. Chem. Eng., **15**: 150-166. 10.1016/S0263-8762(97)80003-2.
- CASNEDE C., COCCO O., MELONI P. & PIA G. (2018) - *Water absorption properties of cement pastes: experimental and modelling inspections.* Adv. Mater. Sci. Eng. Hindawi. <https://doi.org/10.1155/2018/7679131>. Article ID 7679131.
- CASTIGLIONE P., SHOUSE P.J., MOHANTY B., HUDSON D. & GENUCHTEN M.T. (2005) - *Improved tension infiltrometer for measuring low fluid flow rates in unsaturated fractured rock.* Vadose Zone J., **4**(3): 885-890.
- CHANG C.C. & CHENG D.H. (2018) - *Predicting the soil water retention curve from the particle size distribution based on a pore space geometry containing slit-shaped spaces.* Hydrol. Earth Syst. Sci., **22**: 4621-4632.
- CHEN K. & CHEN H. (2020) - *Generalized hydraulic conductivity model for capillary and adsorbed film flow.* Hydrogeol. J., **28**(6): 2259-2274. <https://doi.org/10.1007/s10040-020-02175-1>.
- CHEN H. & FENG S.J. (2023) - *A simple water retention model of dual-porosity soils based on self-similarity of bimodal pore size distribution.* Comput Geotec, **162**: 105684, <https://doi.org/10.1016/j.compgeo.2023.105684>.
- CHEN S., MAO X. & WANG C. (2019) - *A Modified Green-Ampt Model and Parameter Determination for Water Infiltration in Fine-textured Soil with Coarse Interlayer.* Water, **11**: 787. <https://doi.org/10.3390/w11040787>.
- CORRADINI C., MORBIDELLI R., FLAMMINI A. & GOVINDARAJU R.S. (2011) - *A parameterized model for local infiltration in two-layered soils with a more permeable upper layer.* J. Hydrol., **396**(3-4): 221-232.
- CORRADINI C., GOVINDARAJU R.S. & MORBIDELLI R. (2002) - *Simplified modelling of areal average infiltration at the hillslope scale.* Hydrol. Process., **16**(9): 1757-1770.
- COSBY B. J., HORNBERGER G. M., CLAPP R. B. & GINN T. R. (1984), - *A statistical exploration of the relationships of soil moisture characteristics to the physical properties of soils.* Water Resour. Res., **20**: 682-690.
- DUNHAM R.J. (1962) - *Classification of carbonate rocks according to depositional texture.* In: Ham WE (eds) Classification of carbonate rocks a symposium, vol 1. American Ass. Petroleum Geol. Memoir: 108-121.
- EWING R. P. & GUPTA S. C. (1993) - *Modeling percolation properties of random media using a domain network.* Water Resour. Res., **29**: 3169-3178.
- FAZELI M., SHORAFI M., NAMDAR KHOJASTEH D. & PILEVAR SHAHRI A. R. (2010) - *A fractal approach for estimating soil water retention curve.* Journal of Soil Science and Environmental Management, **1**: 177-183.
- FENG Y. & YU B. (2007) - *Fractal dimension for tortuous streamtubes in porous media.* Fractals, **15**(04): 385-390. <https://doi.org/10.1142/S0218348X07003654>.
- FOLK R.L. (1962) - *Spectral subdivision of limestone types.* In: *Classification of carbonate rocks.* A symposium, Memoir 1. (ed.): W.E. Ham, The American Association of Petroleum Geologists, Tulsa, OK: 62-84
- FOLK R.L. (1959) - *Practical petrographic characterization of limestones.* The American Association of Petroleum Geologists Bulletin, **43**: 1-38.
- FRANCUS P. (1998) - *An image-analysis technique to measure grain-size variation in thin sections of soft clastic sediment.* Sed. Geol. **121**(3-4): 289-298.
- FREDLUND M. D., WILSON G. W. & FREDLUND D. G. (2002) - *Use of the grain size distribution for estimation of the soil water characteristic curve.* Can. Geotech. J., **39**: 1103-1117.
- FREDLUND D. G. & A. Q. XING (1994) - *Equations for the soil-water characteristic curve.* Canadian Geotech. Journal, **31**: 521-532.
- GHAMBARIAN-ALAVIJEH B., A. LIAGHAT, G. H. HUANG & M. TH. VAN GENUCHTEN (2010) - *Estimation of the van Genuchten soil water retention properties from soil textural data.* Pedosphere, **20**: 456-465.
- HE CHEN & SHI-JIN FENG (2023) - *A simple water retention model of dual-porosity soils based on self-similarity of bimodal pore size distribution.* Computers and Geotechnics, **162**: 2023, 105684, <https://doi.org/10.1016/j.compgeo.2023.105684>.
- HOFFMAN D. & K. NIESEL (1996) - *Relationship between pore structure and other physic-technical characteristics of stone.* Proceedings 8th Int. Congr. On Deterioration and Conservation of Stone, Berlin, Germany: 461-472.
- HUANG G.H., ZHANG R.D. & HUANG Q.Z. (2006) - *Modeling soil water retention curve with a fractal method.* Pedosphere, **16**: 137-146.
- INTERNATIONAL SOCIETY FOR ROCK MECHANICS (ISRM) - 1979. *Suggested methods for determining water content, porosity, density, absorption and related properties and swelling and slake-durability index properties.* Int. J. Rock Mechanichs Min. Sci. Geomech. Abstr., **16**: 147-159.
- KHODAVERDILOO H, HOMAEI M., VAN GENUCHTEN M. T. & DASHTAKI S. G. (2011) - *Deriving and validating pedotransfer functions for some calcareous soils.* Journal of Hydrology, **399**: 93-99.
- KOSUGI K. (1996) - *Lognormal distribution model for unsaturated soil hydraulic properties.* Water Resour Res., **32**: 2697-2703.
- LENHARD R.J., PARKER J.C. & MISHRA S. (1989) - *On the correspondence between Brooks- Corey and van Genuchten models, 1980.* J. Irrig. Drain. Eng., **115**: 744-751.

- LI D.Q., WANG L., CAO Z.J. & QI X.H. (2019) - *Reliability analysis of unsaturated slope stability considering SWCC model selection and parameter uncertainties*. Eng. Geol., **260**: 105207. <https://doi.org/10.1016/j.enggeo.2019.105207>.
- LIU X. & XU M. (2017) - *The unsaturated hydromechanical coupling model of rock slope considering rainfall infiltration using DDA*. Geofluids. Hindawi: 1-15. <https://doi.org/10.1155/2017/1513421>.
- LU N., KIM T.H., STURE S. & LIKOS W.J. (2009) - *Tensile strength of unsaturated sand*. J. Eng. Mech., **135**(12): 1410-1419.
- LU Z. (2018) - *Sensitivity analysis of hydraulic head to locations of model boundaries*. Water Resour. Res., **54**(2): 1400-1409. <https://doi.org/10.1002/2017WR021955>.
- MINASNY B. & McBRATNEY A. B. (2007) - *Estimating the water retention shape parameter from sand and clay content*. Soil Sci. Soc. Am. J., **71**: 1105-1110.
- MINASNY B., McBRATNEY A.B. & BRISTOW K.L. (1999) - *Comparison of different approaches to the development of pedotransfer functions for water-retention curves*. Geoderma, **93**: 225-253.
- MOHAMMADI M.H. & VANCLOOSTER M. (2011) - *Predicting the Soil moisture characteristic curve from particle size distribution with a simple conceptual model*. Vadose Zone J., **10**(2): 594-602.
- MORBIDELLI R., SALTALIPPI C., FLAMMINI A., CIFRODELLI M., CORRADINI C. & GOVINDARAJU R. S. (2015) - *Infiltration on sloping surfaces: laboratory experimental evidence and implications for infiltration modelling*. J. Hydrol., **523**: 79-85.
- MOREL H. J. & J. NIMMO (1999) - *Soil water retention and maximum capillary drive from saturation to oven Dryness*. Water Resour. Res., **35**: 2031-2041.
- MORGAN J. T. & D. T. GORDON (1970) - *Influence of pore geometry on water-oil relative permeability*. J. Pet. Technol., **22**: 1199-1208.
- NEMES A. & RAWLS W.J. (2004) - *Soil texture and particle-size distribution as input to estimate soil hydraulic properties*. Developments in Soil Science, **30**: 47-70, [https://doi.org/10.1016/S0166-2481\(04\)30004-8](https://doi.org/10.1016/S0166-2481(04)30004-8).
- NG C.W.W. & MENZIES B. (2007) - *Advanced Unsaturated Soil Mechanics and Engineering*. Taylor & Francis, 270 Madison Ave, New York, NY 10016, USA: 712 pp. <https://doi.org/10.1201/9781482266122>
- NG C.W.W. & SHI Q. (1998) - *A numerical investigation of the stability of unsaturated soil slopes subjected to transient seepage*. Comput. Geotech., **22** (1): 1-28.
- NIMMO J.R. (2009) - *Vadose water*. In: Encyclopedia of Inland Waters. Elsevier: 766-777.
- NIMMO J.R. (2005) - *Unsaturated zone flow processes*. In: Anderson, M.G., Bear, J. (Eds.), *Encyclopedia of Hydrological Sciences: Part 13–Groundwater*. Wiley, Chichester, UK: 2299-2322. <https://doi.org/10.1002/0470848944.hsa161>.
- NIMMO J.R. (2004) - *Porosity and pore size distribution*. In: Hillel, D. (Ed.), *Encyclopedia of Soils in the Environment*. Elsevier, London: 295-303.
- NIMMO J.R. & HAMMERMEISTER D. P. (1987) - *Unsaturated flow in a centrifugal field: measurement of hydraulic conductivity and testing of Darcy's law*. Water Resour. Res., **3**(1): 124-134.
- NOVOTNY T.H., DE AZEVEDO E.R., DE GODOY G., CONSALTER D.M. & COOPER M. (2023) - *Determination of soil pore size distribution and water retention curve by internal magnetic field modulation at low field 1H NMR*. Geoderma, **431**: 116363, <https://doi.org/10.1016/j.geoderma.2023.116363>.
- OH S. & LU N. (2015) - *Slope stability analysis under unsaturated conditions: case studies of rainfall-induced failure of cut slopes*. Eng. Geol., **184**: 96-103.
- PASTORE N., CHERUBINI C., DOGLIONI A., GIASI C.I. & SIMEONE V. (2020) - *Modelling of the complex groundwater level dynamics during episodic rainfall events of a surficial aquifer in southern Italy*. Water, **12**(10): 1-21.
- PERFECT E., McLAUGHLIN N.B., KAY B.D. & TOPP G.C. (1996) - *An improved fractal equation for the soil water retention curve*. Water Resour. Res., **32**: 281-287.
- PERRIER E., RIEU M., SPOSITO G. & DE MARSILY G. (1996) - *Models of the water retention curve for soils with a fractal pore size distribution*. Water Resour. Res., **32**: 3025-3031.
- PIRES L. F., CÁSSARO F. A. M., REICHARDT K. & BACCHI O. O. S. (2008) - *Soil porous system changes quantified by analyzing soil water retention curve modifications*. Soil Till. Res., **100**: 72-77.
- RANJBAR A., CHERUBINI C. & PASTORE N. (2022) - *Experimental Investigation on Water Seepage through Transparent Synthetic Rough-Walled Fractures*. Water, **14**: 3199. <https://doi.org/10.3390/w14203199>.
- REYNOLDS W.D., ELRICK D.E. & YOUNGS E.G. (2002) - *Ring or cylinder infiltrometers (Vadose Zone)*. In: J.K. DANE & G. C. TOPP ed. *Method of soil analysis*. Part 4. N. 5.SSSA: 818-826.
- RUSSO D. (1988) - *Determining soil hydraulic properties by parameter estimation: On the selection of a model for the hydraulic properties*. Water Resour. Res., **24**: 453-459.
- SAXTON K. E., W. J. RAWLS, J. S. ROMBERGER & R. I. PAPENDICK (1986) - *Estimating generalized soil-water characteristics from texture*. Soil Sci. Soc. Am. J., **50**: 1031-1036.
- SCHEIDEGGER A.E. (1957) - *The Physics of Flow through Porous Media*. University of Toronto Press, Toronto. <https://doi.org/10.3138/9781487583750>
- SCHNEEBELI M. (1995) - *Development and stability of preferential flow paths in a layered snowpack*. In: *Biogeochemistry of Seasonally Snow-Covered Catchments*. Proc. Boulder Symposium. IAHS Publ.: 89-95.
- TIETJE O. & TAPKENHINRICHS M. (1993) - *Evaluation of pedo-transfer functions*. Soil Sci. Soc. Am. J., **57**: 1088-1095.
- TROPEANO M. & SABATO L. (2000) - *Response of Plio-Pleistocene mixed bioclastic-lithoclastic temperate-water carbonate systems to forced regressions: the Calcarene di Gravina Formation, Puglia SE Italy*. In: HUNT D. & GAWTHORPE R.L. (eds.). "Sedimentary Responses to Forced Regressions", Geologi-

- cal Society, London, Spec. Publ., **172**: 217 -243.
- TURTURRO A.C., CAPUTO M.C., PERKINS K.S. & NIMMO J.R. (2020) - *Does the Darcy- Buckingham Law apply to flow through unsaturated porous rock?* Water, **12**(10): 2668. <https://doi.org/10.3390/w12102668>
- TURTURRO A.C., ANDRIANI G.F., CAPUTO M.C. & MAGGI S. (2013) - *Experimental determination of hydraulic properties of unsaturated calcarenites*. EGU General Assembly Conference Abstracts EGU2013-7862.
- TYLER S.W. & WHEATCRAFT S.W. (1989) - *Application of fractal mathematics to soil water retention estimation*. Soil Sci. Soc. Am. J., **53**: 987-996.
- VAN GENUCHTEN M. T. (1980) - *A closed-form equation for predicting the hydraulic conductivity of unsaturated soils*. Soil Sci. Soc. Am. J., **44**: 892-898.
- VAN GINKEL M. & OLSTHOORN T.N. (2019) - *Distribution of grain size and resulting hydraulic conductivity in land reclamations constructed by bottom dumping, rainbowing and pipeline discharge*. Water Resour Manage, **33**: 993-1012 <https://doi.org/10.1007/s11269-018-2158-3>.
- VEREecken H., J. MAES J. FEYEN & P. DARIUS (1989) - *Estimating the soil moisture retention curve from texture, bulk density, and carbon content*. Soil Sci., **148**: 389-403.
- WANG J.-P., HU N., FRANCOIS B. & LAMBERT P. (2017) - *Estimating water retention curves and strength properties of unsaturated sandy soils from basic soil gradation parameters*. Water Resour. Res., **53**(7): 6069-6088. <https://doi.org/10.1002/2017WR020411>.
- WÖSTEN J. H. M., P. A. FINKE & M. J. W. JANSEN (1995) - *Comparison of class and continuous pedotransfer functions to generate soil hydraulic characteristics*. Geoderma, **66**: 227-237.
- WÖSTEN J. H. M. & M. T. VAN GENUCHTEN (1988) - *Using texture and other soil properties to predict the unsaturated soil hydraulic functions*. Soil Sci. Soc. Am. J., **52**: 1762-1770.
- XIAO T., LI D.Q., CAO Z.J., AU S.K. & PHOON K.K. (2016) - *Three-dimensional slope reliability and risk assessment using auxiliary random finite element method*. Comput. Geotech., **79**: 146-158.
- XU Y. (2004) - *Calculation of unsaturated hydraulic conductivity using a fractal model for the pore-size distribution*. Comput. Geotech., **31**: 549-557.
- YANG S.R. & HUANG L.J. (2023) - *Infiltration and Failure Behavior of an Unsaturated Soil Slope under Artificial Rainfall Model Experiments*. Water, **15**: 1599. <https://doi.org/10.3390/w15081599>
- ZHAN T.L.T. & NG C.W.W. (2004) - *Analytical analysis of rainfall infiltration mechanism in unsaturated soils*. Int. J. Geomech., **4**(4): 273-284. [https://doi.org/10.1061/\(ASCE\)1532-3641\(2004\)4:4\(273\)](https://doi.org/10.1061/(ASCE)1532-3641(2004)4:4(273)).
- ZHOU Q.Y., MATSUI H. & SHIMADA J. (2004) - *Characterization of the unsaturated zone around a cavity in fractured rocks using electrical resistivity tomography*. J. Hydraul. Res., **42** (sup1): 25-31.

Received January 2024 - Accepted March 2024